Received: 27 January 2021 | Revised: 13 August 2021 | Accepted: 13 August 2021

DOI: 10.1002/bit.27915

ARTICLE

BIOTECHNOLOGY AND BIOENGINEERING WILEY

Fast identification of off-target liabilities in early antibiotic discovery with Fourier-transform infrared spectroscopy

Bernardo Ribeiro da Cunha[1,2] | Sandra M. Aleixo[3,4] | Luís P. Fonseca[1] | Cecília R. C. Calado[2,5]

[1]Institute for Bioengineering and Biosciences (iBB), Instituto Superior Técnico (IST), Universidade de Lisboa (UL), Lisboa, Portugal

[2]Área Departamental de Engenharia Química (ADEQ), ISEL-Instituto Superior de Engenharia de Lisboa, Instituto Politécnico de Lisboa, Lisboa, Portugal

[3]Área Departamental de Matemática (ADM), ISEL-Instituto Superior de Engenharia de Lisboa, Instituto Politécnico de Lisboa, Lisboa, Portugal

[4]Centro de Estatística e Aplicações da Universidade de Lisboa (CEAUL), Faculdade de Ciências da Universidade de Lisboa, Campo Grande, Lisboa, Portugal

[5]CIMOSM, ISEL—Centro de Investigação em Modelação e Otimização de Sistemas Multifuncionais, Instituto Superior de Engenharia de Lisboa, Lisboa, Portugal

Correspondence
Bernardo Ribeiro da Cunha, Institute for Bioengineering and Biosciences (iBB), Instituto Superior Técnico (IST), Universidade de Lisboa (UL); Av. Rovisco Pais, 1049-001 Lisboa, Portugal.
Email: bernardo.cunha@tecnico.ulisboa.pt

Funding information
Fundação para a Ciência e a Tecnologia, Grant/Award Number: UIDB/00006/2020; Insituto Politécnico de Lisboa, Grant/Award Numbers: 2018/RenalProg/ISEL, 2020/NephroMD, IDI&CA/IPL/2017/DrugsPlatf/ISEL

Abstract

Structural modifications of known antibiotic scaffolds have kept the upper hand on resistance, but we are on the verge of not having antibiotics for many common infections. Mechanism-based discovery assays reveal novelty, exclude off-target liabilities, and guide lead optimization. For that, we developed a fast and automatable protocol using high-throughput Fourier-transform infrared spectroscopy (FTIRS). Metabolic fingerprints of *Staphylococcus aureus* and *Escherichia coli* exposed to 35 compounds, dissolved in dimethyl sulfoxide (DMSO) or water, were acquired. Our data analysis pipeline identified biomarkers of off-target effects, optimized spectral preprocessing, and identified the top-performing machine learning algorithms for off-target liabilities and mechanism of action (MOA) identification. Spectral bands with known biochemical associations more often yielded more significant biomarkers of off-target liabilities when bacteria were exposed to compounds dissolved in water than DMSO. Highly discriminative models distinguished compounds with predominant off-target effects from antibiotics with well-defined MOA (AUROC > 0.87, AUPR > 0.79, F1 > 0.81), and from the latter predicted their MOA (AUROC > 0.88, AUPR > 0.70, F1 > 0.70). The compound solvent did not affect predictive models. FTIRS is fast, simple, inexpensive, automatable, and highly effective at predicting MOA and off-target liabilities. As such, FTIRS mechanism-based screening assays can be applied for hit discovery and to guide lead optimization during the early stages of antibiotic discovery.

KEYWORDS
Fourier-transform infrared spectroscopy (FTIR), high-throughput screening, machine learning, mechanism of action, off-target liabilities

1 | INTRODUCTION

Thirty years from now, antibiotic-resistant infections will cause the death of more people than cancer does now and carry a cumulative cost of inaction in excess of $100 trillion (O'Neill, 2014). Structural modifications of major antibiotic classes, mostly discovered with the Waksman platform, filled the pipeline and temporarily outpaced resistance (Lewis, 2013), but a discovery void since the late 1980s (Silver, 2011) has put humanity on the verge of not having therapeutic options for many common infections. The challenge is finding novelty with the characteristics that make an ideal antibiotic (Singh et al., 2017), namely high antimicrobial activity and very low toxicity (Rolain & Baquero, 2016). In fact, nearly one-third of drug discovery attrition is due to toxicity (Peter Guengerich, 2011). Antibiotics are toxic due to structural homology between prokaryotes and the host, or other undesirable off-target activity (Rudmann, 2013). Even

candidates with sufficient antimicrobial activity and acceptable cytotoxic profiles might not be suitable for therapeutic use, as in vitro activity often does not correlate with in vivo efficacy. The latter is better understood by elucidating a compound's mechanism of action (MOA) (Pethe et al., 2010). Also, shifting to a mechanism-based discovery approach opens the door to gray chemical matter (Peach et al., 2013), which could provide good candidates for medicinal chemistry programs (Zoffmann et al., 2019). MOA identification can also guide lead optimization by identifying structural modifications that induce predominant off-target activity, that is, toxic compounds (Cunningham et al., 2013). Although MOA identification is not necessary (Silver, 2016), it increases the probability of success of drug discovery programs (Moffat et al., 2017).

Typically, MOA identification involves techniques that are either slow, low-throughput, difficult to scale, costly, labor-intensive or a combination thereof (Briffotaux et al., 2019; Chevereau & Bollenbach, 2015; Cunningham et al., 2013; Ma et al., 2017; Nishiya et al., 2017; Pathania et al., 2009; Phillips et al., 2011; Rock et al., 2007; Zampieri et al., 2017; Zoffmann et al., 2019). Similarly, off-target screening panels are inefficient, and often unpracticable, to monitor safety profiles across successive generations of structural derivatives. Also, these panels are biased toward known mechanisms of toxicity; only probe one off-target interaction; and evaluate the compound itself, not secondary metabolites (Brown et al., 2020). As such, the quest for a fast, cheap, and automatable technique that can be used for the systematic identification of MOA and exclusion of toxic compounds continues. Fourier-transform infrared (FTIR) spectroscopy (FTIRS) is a technique with such characteristics that reflects the vibrational energy of molecular bonds after their interaction with infrared radiation, thereby revealing the atoms participating in said bonds, which in turn conveys the molecular composition of biological samples regarding nucleic acids, proteins, carbohydrates, lipids, phospholipids, among others (Ribeiro da Cunha et al., 2020). FTIRS conveys the molecular composition of samples with sufficient detail that it is suitable for metabolic fingerprinting in general (Goodacre et al., 2004), and specifically for identifying antibiotic-induced profiles (Huleihel et al., 2009; Ribeiro da Cunha et al., 2019, 2020; Xuan Nguyen et al., 2017). Recently, FTIRS has also been shown to be sufficiently sensitive for screening animal DNA polymorphism (Gomes Rios et al., 2021) as well as for detecting single mtDNA deletions, which can enable the diagnosis of mitochondrial myopathy in clinical practice (Gervasoni et al., 2020). In addition, FTIRS sensitivity extends beyond the molecular composition of samples through to their structural and conformational features. Examples of this include protein folding, biomembrane organization, and fluidity, as well as nucleic acid conformation (Ribeiro da Cunha et al., 2020). In this study, an FTIRS assay was developed to capture the metabolic fingerprints induced by antibiotics and chemical stressors on *Staphylococcus aureus* and *Escherichia coli*. The effect of the antibiotic solvent was evaluated by exposing each bacterium to the compounds dissolved in water or dimethyl sulfoxide (DMSO). A data analysis pipeline was implemented to identify biomarkers of off-target effects, optimize spectral preprocessing, and select the top-performing machine learning algorithms for the identification of off-target liabilities and MOA prediction.

2 | MATERIALS AND METHODS

2.1 | High-throughput spectra acquisition

Stock solutions of all compounds (Table S1) were prepared at 6 mM either in water or DMSO (6% v/v). Five independent cultures of *E. coli* (ATCC 33876) and *S. aureus* (ATCC 6538 P) were grown on 90 ml of cation-adjusted Mueller-Hinton broth (VWR, Portugal) at 37°C, 250 rpm until early-exponential phase (~3 h). Bacteria were centrifuged at 3000 RCF for 10 min and resuspended in 6 ml of NaCl 0.9% to obtain an ABS_{600} of 0.75 or 1.5 for *E. coli* and *S. aureus*, respectively. Afterward, cells were dispensed on a 96-well microtiter flat-bottomed polystyrene plate (60 µl/well), previously prepared with 60 µl of 3× concentrated growth media and 60 µl of stock solution. After a 2 h incubation at 37°C, 30 µl were transferred to an infrared transparent ZnSe 96-well plate (Bruker) in triplicate, which corresponded to mechanical replicates. ZnSe plates were dehydrated for 1 h in a vacuum desiccator with abundant silica and inserted in an HTS-XT module coupled to a Vertex-70 spectrometer (Bruker Optics). Spectra were acquired in transmission mode and consisted of 40 coadded scans at a 4 cm^{-1} resolution. Raw spectra were exported from the OPUS software (Bruker) as data point table files into MATLAB (MathWorks) for subsequent analysis.

2.2 | Spectra quality control

Mechanical replicates consistently deemed outliers across different quality control criteria were excluded from the data set. The biofilm thickness, signal-to-noise ratio, and water vapor content were used as quality control criteria (Lasch, 2012). Samples scoring above $q_3 + w \times (q_3 - q_1)$ or below $q_1 + w \times (q_3 - q_1)$, where w is the whisker length (approximately $\pm 2.7\sigma$) and q_1 and q_3 are the 25th and 75th percentiles, for these three quality control criteria, were deemed suspected outliers. If suspected outliers also scored above the 99% confidence limit of a principal component analysis Hoteling's T^2 (Römer et al., 2008) they were considered outliers and removed from the data set. No more than two mechanical replicates were considered outliers for any given sample. Mechanical replicates that passed the quality control routines were averaged, so a single spectrum for each of the five biological replicates was used in subsequent analysis.

2.3 | Statistical analysis for biomarker identification

An automated script was developed, from a previously described workflow (Marques et al., 2019), to identify biomarkers that

distinguish, in mean terms, two populations by applying the most suitable hypothesis tests to the corresponding independent groups of observations. A detailed description is available in the Supporting Information Materials. Parametric tests were preferred as they're more powerful and are more likely to detect true differences. However, if their assumptions are not met, their results are not statistically valid and may lead to inaccurate conclusions, so nonparametric tests should be used (Chan, 2003; Ghasemi & Zahediasl, 2012; Kafadar & Sheskin, 2006; Kaur & Kumar, 2015; Lang, 2004; Neideen & Brasel, 2007). Nonparametric tests were also used when samples had less than 20 observations as goodness-of-fit tests are unlikely to detect non-normality (Noughabi & Arghami, 2011; Romão et al., 2010; Royston, 1995; Yap & Sim, 2011). First, the Shapiro-Wilk test, adjusted by Royston, was used to evaluate normality for samples with at least 20 observations. Then, if both samples came from populations with normal distribution, an *F* test evaluated populational equality of variances. If the population variances were equal, equality of mean population values was evaluated with a two-sample *T* test; otherwise, a Welsh *T* test was applied. If both samples did not come from populations with normal distribution, one of two situations occurred: either both had a size of at least 30, in which case the parametric *Z* test was used to assess the equality of the mean population values, given the central limit theorem; otherwise, both had size less than 30 and the equality of the population medians was evaluated with a non-parametric Mann-Whitney-Wilcoxon test. Lastly, if one of the samples came from a population with normal distribution and the other did not, then either the sample from the non-normal population had less than thirty observations, in which case the non-parametric Mann-Whitney-Wilcoxon test was used, or if the sample from the non-normal population had more than 30 observations, again using the central limit theorem, the parametric *Z* test was used to evaluate the equality of the mean population values. The automated workflow was implemented using MATLAB. Irrespectively of the test used to evaluate the equality of mean or median population values, if the null hypothesis is rejected then, in mean terms, there are significant differences between the groups of observations, and the ratio is considered a biomarker. All tests were applied for a significance level of 5%.

2.4 | Preprocessing optimization and predictive algorithms

Preprocessing aims to reduce the non-discriminatory sample-specific component of the spectra while highlighting inter-replica variability (Randolph, 2006). The most frequently used preprocessing algorithms are the Savitzky-Golay (SG) filter and MSC, either in its extended version (EMSC) or its extended version with replicate correction (EMSCrep) (Martens et al., 2003). EMSCrep was applied using the toolbox provided by Afseth and Kohler (2012). The performance of these algorithms depends on their parametrization, which requires extensive optimization (Zimmermann & Kohler, 2013). For that, a previously described method was used to optimize preprocessing parameters (Ribeiro da Cunha et al., 2021). Machine learning models were created with MATLAB's Classification Learner App using standard parameters and then developed with stand-alone scripts. Briefly, Support Vector Machines (SVM) were used for one-vs-all multiclass classification with either the linear, quadratic, cubic, fine Gaussian, medium Gaussian or coarse Gaussian kernel function applied on standardized data. For fine, medium, and coarse Gaussian, the kernel scale was 11, 43, and 170 respectively, while for the other kernel functions this was set to automatic. All SVM models are considered a box constrain of level 1. K-Nearest Neighbor (KNN) was applied on standardized data using the Euclidean distance with equal weight, considering 1, 10, and 100 neighbors for the fine, medium, and KNN respectively. Both the Cosine and Cubic KNN considered 10 neighbors, while the distance metrics were the Cosine and Minkowski, respectively. Weighted KNN applied squared inverse weights to a Euclidean distance considering 10 neighbors. Additionally, ensemble models of decision trees were determined using both the AdaBoost and RSUBoost method with 30 learners at a rate of 0.1 and 20 splits, and the Bag method, which uses random predictor selections at each split (i.e., random forests) with 30 learners. Subspace ensembles were determined for discriminant analysis and KNN considering a dimension of 14 subspaces and 30 or 1 learner, respectively. The discriminant analysis considered the diagonal covariance matrix. Accuracy was determined as the ratio between the predicted true positives plus the true negatives over the total number of observations. Precision was calculated as the true positive rate over the true positive rate plus the false positive rate. Recall, or sensitivity was determined as the true positive rate over the sum of the true positive rate plus the false-negative rate. Specificity was calculated as the true negative rate over the sum of true negative plus false positives. The receiver operating characteristic (ROC) and precision-recall (PR) curves were calculated using MATLAB's perfcurve function.

3 | RESULTS

3.1 | Compound concentration, exposure duration, library solvent, and other considerations

In addition to expanding the "screenable" chemical space to compounds with lower antimicrobial activity, which are typically excluded in the early stages of activity-based assays, the transition to mechanism-based antibiotic discovery has other advantages. Effectively, focusing first on MOA dismisses the burden of testing a range of concentrations for each compound as identifying high-potency candidates is no longer a prerequisite. Importantly, this does not impair MOA resolution as a large spectrum of MOA can be detected with FTIRS by exposing bacteria to a single concentration (Ribeiro da Cunha et al., 2021). This implies faster and simpler workflows, requiring less compound quantity and other consumables. In addition, because the endpoint is no longer growth inhibition typically observed after 16–24 h, shorter time-frames can be considered. Typically, metabolic profiles of antibiotic exposure are mostly generic

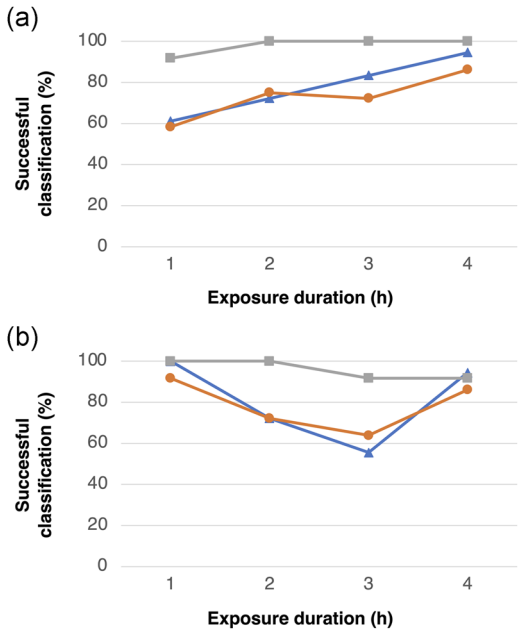

FIGURE 1 Effect of compound concentration and exposure duration on the mechanism of action prediction. Each data point corresponds to the successful classification of a leave-one-out cross-validated partial least squares discriminant analysis of Fourier-transform infrared spectra of *Escherichia coli* (a) and *Staphylococcus aureus* (b), after preprocessing with optimized parameters. Antibiotic concentrations ranged from 1,000 μM (gray squares), 100 μM (orange circles), and 10 μM (blue triangles)

during the initial 30 min, and become more specific 60 min after exposure, and even more so 90 min after exposure (Belenky et al., 2015). These profiles become specific faster if the antibiotic concentration is considerably higher than the minimum inhibitory concentration (Hoerr et al., 2016).

Thus, the effect of compound concentration (10, 100, and 1 mM) and exposure duration (1, 2, 3, and 4 h) on MOA prediction was evaluated (Figure 1). For that, FTIR spectra of *E. coli* and *S. aureus* exposed to amoxicillin and ampicillin, kanamycin, and neomycin, as well as sulfamethazine and sulfamethoxazole, were acquired. Spectral preprocessing was optimized, and MOA was predicted with a Partial Least Squares discriminant analysis (PLS-DA) after Leave-One-Out Cross-Validation (LOO-CV). To ensure bacteria were exposed to the same number of molecules, which is more pharmacologically representative of their relative potency, molar concentrations were used. In fact, these should arguably become the standard dose system (Chmielewska & Lamparczyk, 2008).

A 2 h exposure at the highest concentration was chosen as this ensured perfect MOA prediction for both strains. FTIR spectra of both bacteria were acquired after exposure to 35 compounds (Table S1), 24 of which were antibiotics of 13 classes that act on 6 biosynthetic pathways. Importantly, most major classes used in systemic therapy were included, which are highly desirable by the pharmaceutical industry. Of the remaining compounds, eight were chemical stressors, as examples of compounds predominantly with off-target effects, and two were controls (the distribution of mechanistic categories of the compounds tested is available in Figure S1).

The most commonly used solvent for large compound libraries, DMSO, is known for altering permeability and interfering with reactive oxygen species, which inhibits the rapid killing of some antibiotic classes and increases the potency of others, even at concentrations as low as 1% (Mi et al., 2016). Alternatively, we explored water as a solvent. However, many molecules are not water-soluble in their early stages of development, and although medicinal chemistry programs often improve this (Wu et al., 2020), it could strongly bias the assay. Although a single universal solvent would be preferable for assay simplicity and throughput, all experiments were conducted with both solvents. Interestingly, spectral differences were more noticeable between different solvents than between different bacteria (Figure 2).

In a typical FTIRS protocol, samples are washed, to remove the growth media, and resuspended to a predetermined cell concentration, which yields cleaner FTIR spectra with normalized biochemical constituents. In this study, we opted to skip the washing step. This was done to reduce the number of steps and thereby increase throughput, to ensure the spectra also reflect the extracellular components of the samples, and to avoid nonspecific metabolic alterations induced by washing the samples after compound-induced metabolic alterations, whose reflection on the spectra we wanted to maximize. As such, bacteria were grown to exponential phase, centrifuged, and concentrated to obtain adequate biomass density for spectra acquisition. Only after this step were bacteria incubated with the compound library dissolved in both solvents. After a short incubation, when samples are typically washed, we opted to directly transfer samples to an infrared transparent plate without washing and FTIR spectra were quickly acquired. Due to its simplicity, and given the sample layout was kept the same, our assay was fast and well-suited for automation. Moreover, our assay ensured spectra were acquired from bacteria exposed to the compound library with minimal manipulations, thereby minimizing nonspecific alterations, which we believe yielded more representative metabolic snapshots that resulted in increased MOA resolution. On the downside, this approach meant spectra included a "noise" component, which reflected the growth media composition, along with the compound and its solvent. Although we cannot exclude the effect of this "noise" component on MOA classification, the heterogeny and size of our compound library ensured the robustness of the models presented in this study. For instance, the structural heterogeneity within compounds targeting protein synthesis, for instance, macrolides, aminoglycosides, and tetracycline, did not impede their similar MOA profiles, which suggests these profiles are based not on the presence of the compounds, but rather on their effect on the bacterial metabolism.

3.2 | Biomarkers of off-target effects

Spectral band ratios were built from all combinations of FTIR spectra bands with a well-established biochemical assignment (Maquelin et al., 2002; Ribeiro da Cunha et al., 2020) (Table 1). Before

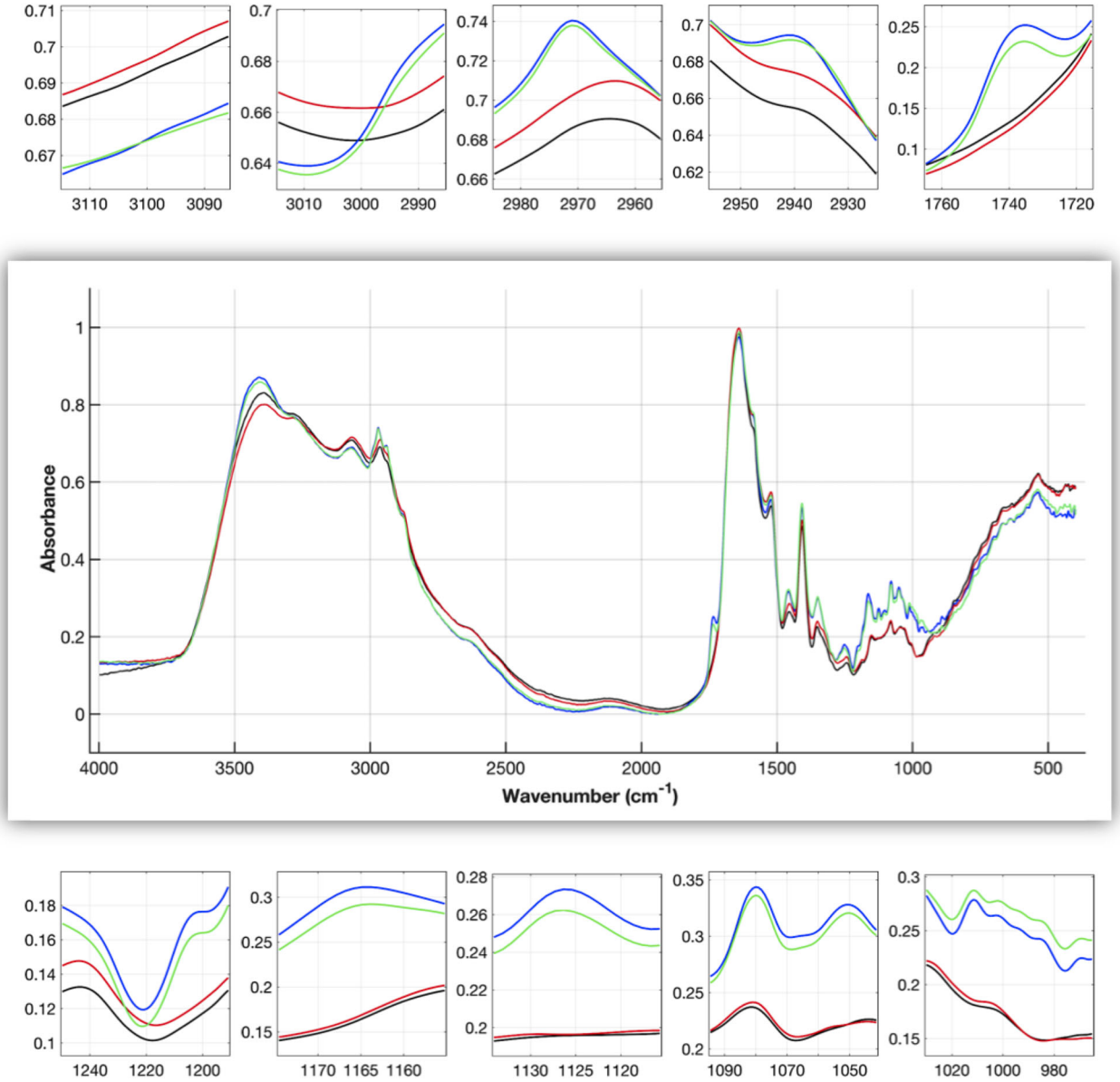

FIGURE 2 Fourier-transform infrared spectra of *Staphylococcus aureus* (black and blue) and *Escherichia coli* (red and green) after exposure to enrofloxacin dissolved in water (black and red) or DMSO (blue and green). Spectra are averages of five biological replicates after preprocessing with baseline correction, normalization and extended multiplicative scatter correction with replicate correction. DMSO, dimethyl sulfoxide

calculating spectral ratios, raw spectra were preprocessed with offset correction and EMSCrep. A total of 870 spectral ratios were analyzed. Of these, spectra of *S. aureus* exposed to compounds dissolved in water yielded 639 biomarkers, and 60 biomarkers when compounds were dissolved in DMSO. Similarly, spectra of *E. coli* exposed to compounds dissolved in water yielded 602 biomarkers and 44 when dissolved in DMSO. Despite the drastic effect of the solvent on the number of ratios that are deemed biomarkers, this alone is not very informative. Therefore, for a given band present in at least one biomarker, the inverse of the *p* value of all biomarkers to which said band contributed was summed. As such, this band importance in biomarker (BIB) score reflects the frequency and weight of a given band across all biomarkers. Bands that more frequently yielded more significant biomarkers presented a higher BIB score. In turn, this allows mapping the spectral origin of the biomarkers for either of the four datasets (Figure 3).

Greater differences in the BIB score were found depending on the compound library solvent than the bacterial model. When water was the solvent, the three most relevant bands were 1380, 1466, and 1455 cm^{-1}, which correspond to the stretching of methyl groups habitually found in lipids; to the asymmetric bending of methyl groups commonly found in lipids and proteins; and the asymmetric bending of methylene groups typically found in lipids and proteins, respectively. However, these bands had a neglectable or zero BIB score when DMSO was the solvent. In this case, the most significant bands were less coherent across both bacterial models. Here, the

TABLE 1 Common biochemical assignments of the vibrational modes detected with Fourier-transform infrared spectroscopy

Wavenumber (cm^{-1})	Vibrational mode	Biochemical assignment
3500	ν(O − H)	
3300	ν(N − H)	Amide A
3100	ν(N − H)	Amide B
2960	$\nu_{as}(CH_3)$	Lipids
2920	$\nu_{as}(CH_2)$	Lipids
2870	$\nu_s(CH_3)$	Lipids
2850	$\nu_s(CH_2)$	Lipids
1740	ν(C = O)	Phospholipid esters
1680		Amide I (antiparallel pleated sheets and α-turns)
1655		Amide I (α-helical structures)
1650	80%ν(CO); 20%ν(C − N)	Amide I
1637	-	Amide I (β-pleated -sheet structures)
1550	60%γ(N − H); 30%ν(C − N); 10%ν(C − C)	Amide II
1515		Tyrosine
1466	$\delta_{as}(CH_3)$	Lipids and proteins
1455	$\delta_{as}(CH_2)$	Lipids and proteins
1380	$\nu(CH_3)$	Phospholipids, fatty acids, triglycerides
1240	$\nu_{as}(PO_2^-)$	DNA, RNA, phospholipid, phosphorylated protein
1150	ν(CO), γ(COH)	Carbohydrates
1120	ν(C − O)	RNA ribose
1111	ν(C − O)	RNA ribose
1080	$\nu_s(PO_2^-)$	DNA, RNA, phospholipid, phosphorylated proteins
1050	ν(COP)	Phosphate ester
1030	*def*(CHO)	Carbohydrates
1012	ν(CO)	DNA and RNA ribose
965	$\nu(PO_3^{2-})$	DNA and RNA
950	$\nu(PO_3^{2-})$	Phosphorylated proteins
920	ν(COP)	Phosphorylated proteins
841		Fingerprint region
620		Fingerprint region

Note: Vibrational modes: ν, stretching; γ, wagging, twisting, and rocking; δ, bending; and *def*, deformation. Where *as*, asymmetrical and *s*, symmetrical.

three most relevant bands were 1680, 3100, and 2920 cm^{-1} for *S. aureus* or 1120 cm^{-1} for *E. coli*. These bands are typically associated with antiparallel pleated sheets and α-turns of Amide I; the stretching of the N–H bond of Amide B; the asymmetric stretching of methylene groups associated with lipids, or the stretching of the C–O bond typically found in RNA ribose, respectively. Moreover, for the same solvent, *S. aureus* spectral ratios yielded more biomarkers than those of *E. coli*. In theory, an experimental protocol that is sensitive to a wider range of metabolic alterations, which in this case translates to higher BIB scores, should be better suited for the fast exclusion of

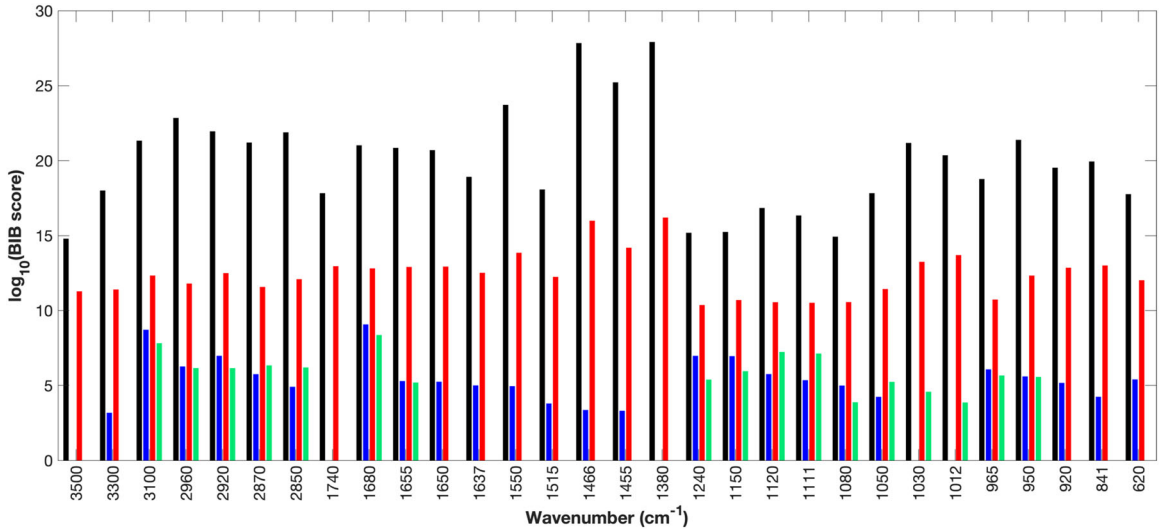

FIGURE 3 BIB scores revealing the contribution of biochemically relevant spectral bands to all identified biomarkers of off-target effects, that is, spectral ratios with statistically significant differences in mean terms, for FTIR spectra of *Staphylococcus aureus* (black and blue) and *Escherichia coli* (red and green) exposed to the compound library dissolved in water (black and red) or DMSO (blue and green). BIB, band importance in biomarker; DMSO, dimethyl sulfoxide; FTIR, Fourier-transform infrared

compounds with off-target effects. However, in a practical sense, this proposition is only useful if it can be validated in a predictive scenario.

3.3 | Distinguishing on- and off-target effects

To evaluate the ability of the proposed assay in predicting off-target effects, various machine learning algorithms were applied to spectra preprocessed with optimized parameters. As EMSCrep combined with second derivative filtering was revealed consistently superior to other forms of MSC and derivative orders, other combinations were not considered during preprocessing optimization. The optimized preprocessing parametrization was identified (Figure S2) for each data set, that is, spectra of *S. aureus* exposed to compounds dissolved in water, spectra of *S. aureus* exposed to compounds dissolved in DMSO, and likewise for *E. coli*. Moreover, the PLS-DA models built for preprocessing optimization revealed uninformative spectral regions (i.e., VIP score <1), which were removed to obtain more robust models and further reduce computation time.

Then, various parametrizations of different machine learning algorithms were applied to each data set, whose accuracy of LOO-CV samples was generally coherent within each data set (Table S2). Minimizing computation time was important as this allowed increasing the number of folds for subsequent cross-validation, which is advantageous as it translates to more training samples that better reflect the underlying sample distribution. Although external validation is widely regarded as a more suitable method to estimate the predictive capability of a given model, it is highly dependent on the random data splits, often yielding unstable estimates. In addition, LOO-CV has been shown to perform better than other *k*-fold and external validation algorithms when dealing with small-sample high-dimensional chemometric data (Majumdar & Basak, 2018).

As such, each sample was predicted exactly once using the most accurate algorithm for its data set, and the posterior probability that it belongs to the positive class, that is, predominant off-target effects, was used to construct the ROC and PR curves shown on Figure 4a,b, from which the F1-score was determined across a range of decision cut-offs (Figure 4c). Although ROC curves are typically used to evaluate a classifiers' performance across decision thresholds, PR curves are often more informative when the data is skewed (Davis & Goadrich, 2016) or when there are few positive cases (Bleakley et al., 2007). Similarly, the F1-score was determined as it provides an estimation of accuracy in a way that is less sensitive to class imbalances, and because it penalizes extreme values.

These indicators revealed that using the same solvent, slightly better predictions were obtained with the *E. coli* datasets than with the *S. aureus* datasets. Moreover, for the *E. coli* data set, using water as a solvent for the compound library yielded marginally better performance, although the opposite occurred with the *S. aureus* data set. It is also interesting to note that the F1 scores follow a similar trend as FTIR spectra, that is, higher similarities were found between different bacteria exposed to the same solvent than between the same bacteria exposed to different solvents. Most importantly, neither the compound library solvent nor the bacterial model, had a drastic effect on the ability to distinguish on-and off-target effects, as could be expected considering the observed BIB scores. In the end, the coherent performance indicators suggest that FTIR spectra provide a sufficiently unique phenotypic fingerprint that enables the fast distinction between bacteria exposed to compounds with predominant off-target effects from those exposed to antibiotics with a well-defined MOA.

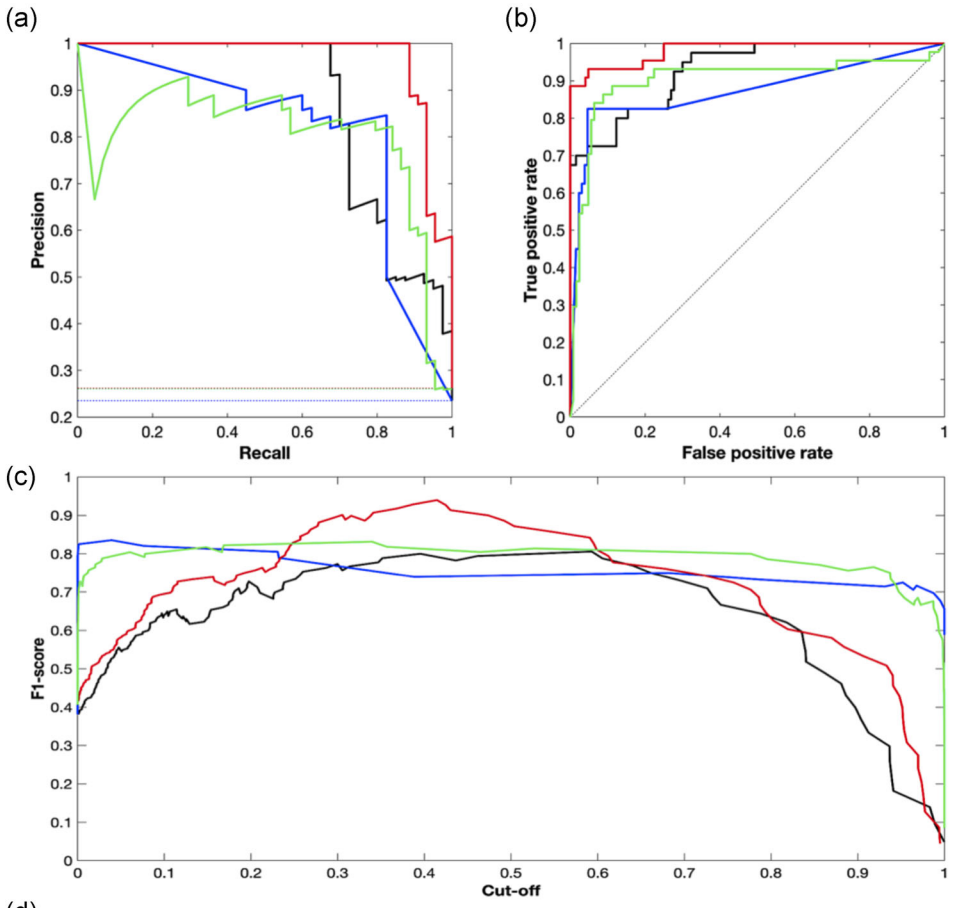

(d)

Dataset	Window size	Polynomial order	Derivative order	Machine learning algorithm	Area under the ROC curve	Area under the PR curve	Maximum F1-score
S. aureus (H_2O)	137	2	2	Ensemble discriminant	0.9304	0.8672	0.8060
S. aureus (DMSO)	29	2	2	SVM quadratic	0.8737	0.8113	0.8354
E. coli (H_2O)	81	2	2	Ensemble discriminant	0.9822	0.9671	0.9398
E. coli (DMSO)	62	4	2	SVM quadratic	0.9022	0.7948	0.8315

FIGURE 4 Ability to distinguish antibiotics with well-defined MOA from compounds with predominant off-target effects. The precision-recall curve (a), along the receiver operating characteristic curve (b), and the F1-score across different decision cut-offs (c) were determined after leave-one-out cross-validation. Machine learning was applied to FTIR spectra of *Staphylococcus aureus* (black and blue), and *Escherichia coli* (red and green) exposed to the compound library dissolved in water (black and red) or DMSO (blue and green) after preprocessing with optimized parameters (d). DMSO, dimethyl sulfoxide; MOA, mechanism of action

3.4 | Guiding medicinal chemistry programs: fast classification of antibiotics MOA

In addition to distinguishing on- versus off-target activity, the fast identification of off-target liabilities can also be achieved by probing the mechanistic category of antibiotics. For that, the optimized preprocessing parameters, followed by removing uninformative spectral regions, used for distinguishing on- and off-target effects, were used. The most accurate machine learning algorithm, and its parameters, was identified for each data set after LOO-CV (Table S3), which in this case were ensembles of subspace discriminant classifiers across the four datasets.

Due to the fast classification of antibiotics MOA is a multiclass prediction problem, a one-versus-all approach was used. As such, ROC and PR curves, as well as F1 scores, were determined for each MOA (Figure S3). Figure 5 presents the area under each curve, as well as the maximum F1-score obtained for each MOA category, and for each data set. Here, it seems that the MOA involving the inhibition of folic acid, mycolic acid and RNA were more challenging to predict. Although this mechanism-specific underperformance was evident in the area under the ROC curve (Figure 4a), it was not as notorious in the area under the PR curve and maximum F-score (Figure 5b,c). One possible reason for this is that the latter are less sensitive to class imbalances and skewed datasets,

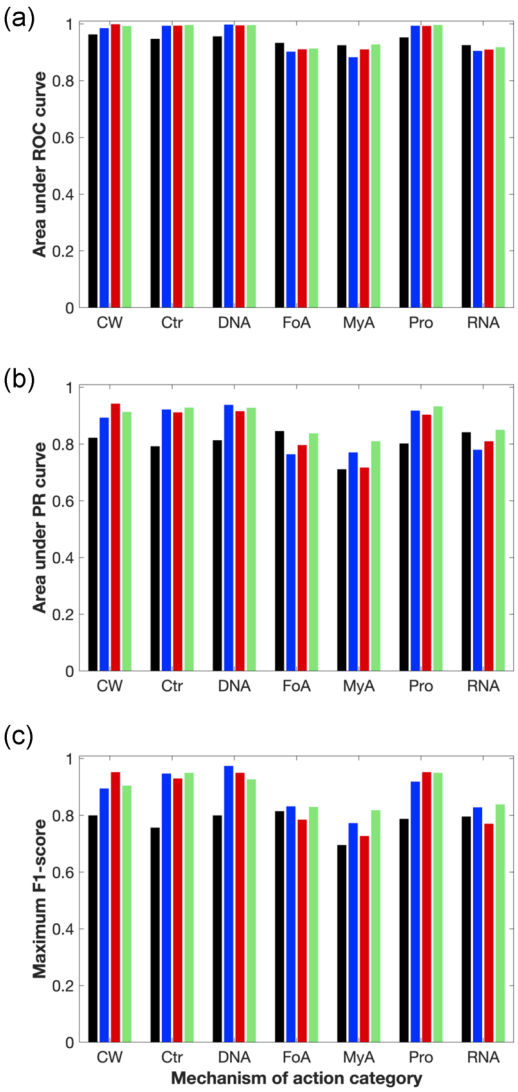

FIGURE 5 Ability to predict antibiotic mechanistic categories, namely those that target the CW, DNA, FoA, MyA, Pro, RNA, and Ctr. The area under the PR curve (a), as well as under the ROC curve (b), along the maximum F1-score (c) were determined with leave-one-out cross-validation of ensembles of subspace discriminant classifiers applied to FTIR spectra of *Staphylococcus aureus* (black and blue) and *Escherichia coli* (red and green) exposed to the compound library dissolved in water (black and red) or DMSO (blue and green) after preprocessing with optimized parameters. CW, cell wall; Ctr, control; DMSO, dimethyl sulfoxide; FoA, folic acid; MyA, mycolic acid; PR, precision-recall; Pro, protein; ROC, receiver operating characteristic

and therefore provided a more accurate description of the models' performance, which were overestimated by the ROC curves. Alternatively, since these were the mechanistic categories with fewer representative antibiotics, it could be that this mechanism-specific underperformance was due to class under-representation. However, the fact that there were as many representatives of the control category as those of the RNA category suggests otherwise.

Moreover, it could also be that these MOA are in fact more challenging to predict. For instance, the inhibition of folic acid by sulfonamides induces a thymineless death, whose mechanism could be similar to a stalled replication fork (Kuong & Kuzminov, 2010), in which case it would resemble the MOA of other DNA synthesis inhibitors such as fluoroquinolones. Similarly, the MOA of isoniazid, which is assumed to be related to the inhibition of mycolic acid synthesis, also impairs the electron transport chain via the accumulation of reactive oxygen species (Zeng et al., 2019). These have been shown to be correlated with the bactericidal activity of various antibiotics (Belenky et al., 2015), and could therefore yield fingerprints where unspecific response mechanisms overshadow antibiotic-specific events, which could result in poorer MOA prediction.

In general, the models constructed were well suited for the fast classification of antibiotics MOA. As no single data set outperformed the remainder, neither the model bacteria nor solvent had a substantial effect on the global predictive performance, as observed for the distinction of on- versus off-target effects. Ultimately, this suggests that phenotypic fingerprints acquired with FTIRS capture the complex biological response when bacteria are exposed to antibiotics of different mechanistic categories and can be used to accurately predict their MOA beyond a given bacterial model or compound library solvent.

4 | DISCUSSION

FTIRS has been shown to detect antibiotic-induced profiles that elucidate their MOA (Huleihel et al., 2009; Ribeiro da Cunha et al., 2019, 2020; Xuan Nguyen et al., 2017). In addition to the prediction of both known and simulated novel MOA, we have shown that FTIRS can be used to estimate potency and to probe the gray chemical matter (Ribeiro da Cunha et al., 2021). In this study, we developed and streamlined a protocol for the fast exclusion of off-target liabilities. This involved minimizing the number of steps, and reducing their duration while ensuring accurate MOA identification. As such, our assay required short cultivation, exposure, sample dehydration, and FTIR spectra acquisition. This means that from frozen bacterial stocks all the way through to exported spectra files took less than 12 h, with a hands-on time around 1 h. In comparison, a streamlined high-throughput metabolomics protocol took at least 2 full days (Zampieri et al., 2018).

First, we developed an automated workflow comprised of a series of hypothesis tests to determine the BIB score of the spectral bands with common biochemical associations. This confirmed that FTIR spectra had intrinsic patterns that reflect the different biological phenomena occurring when bacteria are exposed to antibiotics versus those that occur upon exposure to chemical stressors. Importantly, this was a good starting point before machine learning techniques, whose interpretation becomes increasingly complex as algorithms rely on abstract mathematical relationships to extract patterns that are "suggested" by the user, thereby blurring the relationship between data and biological events.

Then, optimally preprocessed FTIR spectra were analyzed with different machine learning classifiers to predict on- and off-target

effects. Our data analysis pipeline ensured that the sample-specific spectral component was highlighted for each data set, and the most accurate machine learning algorithm was applied. As such, robust performance indicators of different nature, that is, the area under the ROC and PR curves, along the F1-score were achieved for each data set. The same data analysis pipeline was applied to predict the MOA of the previously identified antibiotics, and notwithstanding a slight performance hit, the resulting models were successful in predicting MOA across the mechanistic categories tested. Although larger compound libraries need to be considered, FTIRS seems to be well suited to rapidly distinguish metabolic profiles induced by chemical stressors from the profiles induced by antibiotics with well-defined MOA, and from the latter predict their mechanistic category.

It is interesting to note that visual inspection of the spectra revealed greater similarities between *E. coli* and *S. aureus* exposed to enrofloxacin dissolved in each of the solvents, than between spectra of either bacterium exposed to the antibiotic dissolved in different solvents. This suggests that the solvent affected the specific antibiotic-induced metabolic alterations. This observation was coherent with the spectral bands that most often, and with greater significance, contributed to biomarkers of off-target effects from which we hypothesized that the experimental setup that reveals a wider range of statistically significant biochemical alterations should be better suited for the fast exclusion of compound with off-target effects. However, neither the compound library solvent nor the bacterial model had a drastic effect on the ability to distinguish on- and off-target effects or to predict the MOA of the antibiotics tested. This is particularly relevant because other techniques are sensitive to the metabolic effect of DMSO (Hoerr et al., 2016); as FTIRS is not, it avoids additional steps to stabilize the metabolism that are often not sufficient to avoid divergent metabolic profiles across similar samples, which degrades the quality of MOA profiles and subsequent predictive models.

This suggests that FTIRS is a robust technique that could be used for the rapid exclusion of compounds with predominant off-target activity, and simultaneously provides valuable insight into the MOA of compounds, even if only at the level of the major biosynthetic pathway. This level of sensitivity has proven to be sufficient to guide lead optimization (Cunningham et al., 2013); for example, it is equivalent to macromolecular accumulation assays, whose utility is not to pinpoint MOA, but rather as a simple and fast preliminary screening assay. As our protocol is fast, simple, inexpensive, and highly automatable, it can be used to monitor MOA profiles and thereby rapidly exclude off-target liabilities, which typically arise during medicinal chemistry efforts, before considerable efforts are put into their development and optimization. As such, FTIRS can fuel a new generation of mechanism-based screening assays that could be an invaluable tool for the early stages of antibiotic discovery.

ACKNOWLEDGMENTS

The authors would like to acknowledge the contribution of Ana Linhares Correia to the data collection process. This study was supported by Instituto Politécnico de Lisboa (grants IDI&CA/IPL/2017/DrugsPlatf/ISEL, 2018/RenalProg/ISEL, and 2020/NephroMD) and was partially conducted in the Engineering & Health Laboratory, established through a collaboration between Universidade Católica Portuguesa and Instituto Politécnico de Lisboa. Sandra M. Aleixo was partly supported by the Fundação para a Ciência e Tecnologia, under Grant UIDB/00006/2020 to CEAUL.

CONFLICT OF INTERESTS

The authors declare that there are no conflict of interests.

DATA AVAILABILITY STATEMENT

Data available on request from the authors.

REFERENCES

Afseth, N. K., & Kohler, A. (2012). Extended multiplicative signal correction in vibrational spectroscopy, a tutorial. *Chemometrics and Intelligent Laboratory Systems*, *117*, 92–99. https://doi.org/10.1016/j.chemolab.2012.03.004

Belenky, P., Ye, J. D., Porter, C. B. M., Cohen, N. R., Lobritz, M. A., Ferrante, T., & Collins, J. J. (2015). Bactericidal antibiotics induce toxic metabolic perturbations that lead to cellular damage. *Cell Reports*, *13*(5), 968–980. https://doi.org/10.1016/j.celrep.2015.09.059

Bleakley, K., Biau, G., & Vert, J. P. (2007). Supervised reconstruction of biological networks with local models. *Bioinformatics*, *23*(13), 57–65. https://doi.org/10.1093/bioinformatics/btm204

Briffotaux, J., Liu, S., & Gicquel, B. (2019). Genome-wide transcriptional responses of *Mycobacterium* to antibiotics. *Frontiers in Microbiology*, *10*, 1–14. https://doi.org/10.3389/fmicb.2019.00249

Brown, D. G., Smith, G. F., & Wobst, H. J. (2020). Promiscuity of in vitro secondary pharmacology assays and implications for lead optimization strategies. *Journal of Medicinal Chemistry*, *63*(12), 6251–6275. https://doi.org/10.1021/acs.jmedchem.9b01625

Chan, Y. H. (2003). Biostatistics 102: Quantitative data—Parametric. *Significance*, *44*(8), 391–396.

Chevereau, G., & Bollenbach, T. (2015). Systematic discovery of drug interaction mechanisms. *Molecular Systems Biology*, *11*(4), 807. https://doi.org/10.15252/msb.20156098

Chmielewska, A., & Lamparczyk, H. (2008). Mass versus molar doses, similarities and differences. *Pharmazie*, *63*(11), 843–848. https://doi.org/10.1691/ph.2008.8578

Cunningham, M. L., Kwan, B. P., Nelson, K. J., Bensen, D. C., & Shaw, K. J. (2013). Distinguishing on-target versus off-target activity in early antibacterial drug discovery using a macromolecular synthesis assay. *Journal of Biomolecular Screening*, *18*(9), 1018–1026. https://doi.org/10.1177/1087057113487208

Davis, J., & Goadrich, M. (2016). The relationship between precision-recall and ROC curves. *Proceedings of the 23rd International Conference on Machine Learning*, pp. 233–240. https://doi.org/10.1145/1143844.1143874

Gervasoni, J., Primiano, A., Marini, F., Sabino, A., Biancolillo, A., Calvani, R., & Primiano, G. (2020). Fourier-transform infrared spectroscopy of skeletal muscle tissue: Expanding biomarkers in primary mitochondrial myopathies. *Genes*, *11*(12), 1–8. https://doi.org/10.3390/genes11121522

Ghasemi, A., & Zahediasl, S. (2012). Normality tests for statistical analysis: A guide for non-statisticians. *International Journal of Endocrinology and Metabolism*, *10*(2), 486–489. https://doi.org/10.5812/ijem.3505

Gomes Rios, T., Larios, G., Marangoni, B., Oliveira, S. L., Cena, C., & Alberto do Nascimento Ramos, C. (2021). FTIR spectroscopy with machine learning: A new approach to animal DNA polymorphism screening. *Spectrochimica Acta, Part A: Molecular and Biomolecular Spectroscopy*, *261*, 1–7. https://doi.org/10.1016/j.saa.2021.120036

Goodacre, R., Vaidyanathan, S., Dunn, W. B., Harrigan, G. G., & Kell, D. B. (2004). Metabolomics by numbers: Acquiring and understanding global metabolite data. *Trends in Biotechnology*, *22*(5), 245–252. https://doi.org/10.1016/j.tibtech.2004.03.007

Hoerr, V., Duggan, G. E., Zbytnuik, L., Poon, K. K. H., Große, C., Neugebauer, U., & Vogel, H. J. (2016). Characterization and prediction of the mechanism of action of antibiotics through NMR metabolomics. *BMC Microbiology*, *16*(1), 1–14. https://doi.org/10.1186/s12866-016-0696-5

Huleihel, M., Pavlov, V., & Erukhimovitch, V. (2009). The use of FTIR microscopy for the evaluation of anti-bacterial agents activity. *Journal of Photochemistry and Photobiology, B: Biology*, *96*(1), 17–23. https://doi.org/10.1016/j.jphotobiol.2009.03.009

Kafadar, K., & Sheskin, D. J. (2006). Handbook of parametric and nonparametric statistical procedures, *The American statistician* (Vol. 51). Taylor & Francis. https://doi.org/10.2307/2685909

Kaur, A., & Kumar, R. (2015). Comparative analysis of parametric and non-parametric tests. *Journal of Computer and Mathematical Sciences*, *6*(6), 336–342.

Kuong, K. J., & Kuzminov, A. (2010). Stalled replication fork repair and misrepair during thymineless death in *Escherichia coli*. *Genes to Cells: Devoted to Molecular & Cellular Mechanisms*, *15*(6), 619–634. https://doi.org/10.1111/j.1365-2443.2010.01405.x

Lang, T. (2004). Twenty statistical errors even you can find in biomedical research articles. *Croatian Medical Journal*, *45*(4), 361–370. https://doi.org/10.1007/s10270-014-0435-z

Lasch, P. (2012). Spectral pre-processing for biomedical vibrational spectroscopy and microspectroscopic imaging. *Chemometrics and Intelligent Laboratory Systems*, *117*, 100–114. https://doi.org/10.1016/j.chemolab.2012.03.011

Lewis, K. (2013). Platforms for antibiotic discovery. *Nature Reviews Drug Discovery*, *12*(5), 371–387. https://doi.org/10.1038/nrd3975

Ma, W., Zhang, D., Li, G., Liu, J., He, G., Zhang, P., & Liang, S. (2017). Antibacterial mechanism of daptomycin antibiotic against *Staphylococcus aureus* based on a quantitative bacterial proteome analysis. *Journal of Proteomics*, *150*, 242–251. https://doi.org/10.1016/j.jprot.2016.09.014

Majumdar, S., & Basak, S. C. (2018). Beware of external validation!—A comparative study of several validation techniques used in QSAR modelling. *Current Computer-Aided Drug Design*, *14*(4), 284–291. https://doi.org/10.2174/1573409914666180426144304

Maquelin, K., Kirschner, C., Choo-Smith, L. P., Van Den Braak, N., Endtz, H. P., Naumann, D., & Puppels, G. J. (2002). Identification of medically relevant microorganisms by vibrational spectroscopy. *Journal of Microbiological Methods*, *51*(3), 255–271. https://doi.org/10.1016/S0167-7012(02)00127-6

Marques, V., Cunha, B., Couto, A., Sampaio, P., Fonseca, L. P., Aleixo, S., & Calado, C. R. C. (2019). Characterization of gastric cells infection by diverse *Helicobacter pylori* strains through Fourier-transform infrared spectroscopy. *Spectrochimica Acta, Part A: Molecular and Biomolecular Spectroscopy*, *210*, 193–202. https://doi.org/10.1016/j.saa.2018.11.001

Martens, H., Nielsen, J. P., & Engelsen, S. B. (2003). Light scattering and light absorbance separated by extended multiplicative signal correction. Application to near-infrared transmission analysis of powder mixtures. *Analytical Chemistry*, *75*(3), 394–404. https://doi.org/10.1021/ac020194w

Mi, H., Wang, D., Xue, Y., Zhang, Z., Niu, J., Hong, Y., & Zhao, X. (2016). Dimethyl sulfoxide protects *Escherichia coli* from rapid antimicrobial-mediated killing. *Antimicrobial Agents and Chemotherapy*, *60*(8), 5054–5058. https://doi.org/10.1128/AAC.03003-15.Address

Moffat, J. G., Vincent, F., Lee, J. A., Eder, J., & Prunotto, M. (2017). Opportunities and challenges in phenotypic drug discovery: An industry perspective. *Nature Reviews Drug Discovery*, *16*(8), 531–543. https://doi.org/10.1038/nrd.2017.111

Neideen, T., & Brasel, K. (2007). Understanding statistical tests. *Journal of surgical education*, *64*(2), 93–96. https://doi.org/10.1016/j.jsurg.2007.02.001

Nishiya, Y., Hamada, T., Abe, M., Takashima, M., Tsutsumi, K., & Okawa, K. (2017). A new efficient method of generating photoaffinity beads for drug target identification. *Bioorganic and Medicinal Chemistry Letters*, *27*(4), 834–840. https://doi.org/10.1016/j.bmcl.2017.01.021

Noughabi, H. A., & Arghami, N. R. (2011). Monte carlo comparison of seven normality tests. *Journal of Statistical Computation and Simulation*, *81*(8), 965–972. https://doi.org/10.1080/00949650903580047

O'Neill, J. (2014, December). *Antimicrobial resistance: Tackling a crisis for the health and wealth of nations/The review on antimicrobial resistance chaired by J O'Neil*. Wellcome Trust and the UK Government. https://doi.org/10.1038/510015a

Pathania, R., Zlitni, S., Barker, C., Das, R., Gerritsma, D. A., Lebert, J., & Brown, E. D. (2009). Chemical genomics in *Escherichia coli* identifies an inhibitor of bacterial lipoprotein targeting. *Nature Chemical Biology*, *5*, 849. https://doi.org/10.1038/nchembio.221

Peach, K. C., Bray, W. M., Winslow, D., Linington, P. F., & Linington, R. G. (2013). Mechanism of action-based classification of antibiotics using high-content bacterial image analysis. *Molecular BioSystems*, *9*(7), 1837–1848. https://doi.org/10.1039/c3mb70027e

Peter Guengerich, F. (2011). Mechanisms of drug toxicity and relevance to pharmaceutical development. *Drug metabolism and pharmacokinetics*, *26*(1), 3–14. https://doi.org/10.1016/j.physbeh.2017.03.040

Pethe, K., Sequeira, P. C., Agarwalla, S., Rhee, K., Kuhen, K., Phong, W. Y., & Dick, T. (2010). A chemical genetic screen in *Mycobacterium tuberculosis* identifies carbon-source-dependent growth inhibitors devoid of in vivo efficacy. *Nature Communications*, *1*(1), 1–8. https://doi.org/10.1038/ncomms1060

Phillips, J. W., Goetz, M. A., Smith, S. K., Zink, D. L., Polishook, J., Onishi, R., & Singh, S. B. (2011). Discovery of kibdelomycin, a potent new class of bacterial type II topoisomerase inhibitor by chemical-genetic profiling in *Staphylococcus aureus*. *Chemistry and Biology*, *18*(8), 955–965. https://doi.org/10.1016/j.chembiol.2011.06.011

Randolph, T. W. (2006). Scale-based normalization of spectral data. *Cancer Biomarkers*, *2*(3–4), 135–144. https://doi.org/10.3233/CBM-2006-23-405

Ribeiro da Cunha, B., Fonseca, L. P., & Calado, C. R. C. (2019). A phenotypic screening bioassay for *Escherichia coli* stress and antibiotic responses based on Fourier-transform infrared (FTIR) spectroscopy and multivariate analysis. *Journal of Applied Microbiology*, *127*(6), 1776–1789. https://doi.org/10.1111/jam.14429

Ribeiro da Cunha, B., Fonseca, L. P., & Calado, C. R. C. (2020). Metabolic fingerprinting with fourier-transform infrared (FTIR) spectroscopy: Towards a high-throughput screening assay for antibiotic discovery and mechanism-of-action elucidation. *Metabolites*, *10*(4), 145. https://doi.org/10.3390/metabo10040145

Ribeiro da Cunha, B., Fonseca, L. P., & Calado, C. R. C. (2021). Simultaneous elucidation of antibiotic mechanism of action and potency with high-throughput Fourier-transform infrared (FTIR) spectroscopy and machine learning. *Applied Microbiology and Biotechnology*, *105*(3), 1269–1286. https://doi.org/10.1007/s00253-021-11102-7

Ribeiro da Cunha, B., Ramalhete, L., Fonseca, L. P., & Calado, C. R. C. (2020). Fourier-transform mid-infrared (FT-MIR) spectroscopy in biomedicine. In Y. Tutar (Ed.), *Essential techniques for medical and life scientists: A guide to contemporary methods and current applications—Part II* (pp. 1–39). Bentham Science Publishers. https://doi.org/10.2174/9789811464867120010004

Rock, F. L., Mao, W., Yaremchuk, A., Tukalo, M., Crépin, T., Zhou, H., & Alley, M. R. K. (2007). An antifungal agent inhibits an aminoacyl-tRNA synthetase by trapping tRNA in the editing site. *Science*, *316*(5832), 1759–1761. https://doi.org/10.1126/science.1142189

Rolain, J. M., & Baquero, F. (2016). The refusal of the society to accept antibiotic toxicity: Missing opportunities for therapy of severe infections. *Clinical Microbiology and Infection*, *22*(5), 423–427. https://doi.org/10.1016/j.cmi.2016.03.026

Romão, X., Delgado, R., & Costa, A. (2010). An empirical power comparison of univariate goodness-of-fit tests for normality. *Journal of Statistical Computation and Simulation*, *80*(5), 545–591. https://doi.org/10.1080/00949650902740824

Royston, P. (1995). A remark on algorithm as 181: The W-test for normality. *Journal of the Royal Statistical Society: Series C, Applied Statistics*, *44*(4), 547–551. https://doi.org/10.2307/2986146

Rudmann, D. G. (2013). On-target and off-target-based toxicologic effects. *Toxicologic Pathology*, *41*(2), 310–314. https://doi.org/10.1177/0192623312464311

Römer, M., Heinämäki, J., Strachan, C., Sandler, N., & Yliruusi, J. (2008). Prediction of tablet film-coating thickness using a rotating plate coating system and NIR spectroscopy. *AAPS PharmSciTech*, *9*(4), 1047–1053. https://doi.org/10.1208/s12249-008-9142-9

Silver, L. L. (2011). Challenges of antibacterial discovery. *Clinical Microbiology Reviews*, *24*(1), 71–109. https://doi.org/10.1111/j.1749-6632.2010.05828.x

Silver, L. L. (2016). Appropriate targets for antibacterial drugs. *Cold Spring Harbor Perspectives in Medicine*, *6*(12), 1–7. https://doi.org/10.1101/cshperspect.a030239

Singh, S. B., Young, K., & Silver, L. L. (2017). What is an "ideal" antibiotic? Discovery challenges and path forward. *Biochemical Pharmacology*, *133*, 63–73. https://doi.org/10.1016/j.bcp.2017.01.003

Wu, Y., Ding, X., Yang, Y., Li, Y., Qi, Y., Hu, F., & Zhao, Y. (2020). Optimization of biaryloxazolidinone as promising antibacterial agents against antibiotic-susceptible and antibiotic-resistant gram-positive bacteria. *European Journal of Medicinal Chemistry*, *185*, 111781. https://doi.org/10.1016/j.ejmech.2019.111781

Xuan Nguyen, N. T., Sarter, S., Hai Nguyen, N., & Daniel, P. (2017). Detection of molecular changes induced by antibiotics in Escherichia coli using vibrational spectroscopy. *Spectrochimica Acta—Part A: Molecular and Biomolecular Spectroscopy*, *183*, 395–401. https://doi.org/10.1016/j.saa.2017.04.077

Yap, B. W., & Sim, C. H. (2011). Comparisons of various types of normality tests. *Journal of Statistical Computation and Simulation*, *81*(12), 2141–2155. https://doi.org/10.1080/00949655.2010.520163

Zampieri, M., Sekar, K., Zamboni, N., & Sauer, U. (2017). Frontiers of high-throughput metabolomics. *Current Opinion in Chemical Biology*, *36*, 15–23. https://doi.org/10.1016/j.cbpa.2016.12.006

Zampieri, M., Szappanos, B., Buchieri, M. V., Trauner, A., Piazza, I., Picotti, P., & Sauer, U. (2018). High-throughput metabolomic analysis predicts mode of action of uncharacterized antimicrobial compounds. *Science Translational Medicine*, *10*, 1–12. https://doi.org/10.1126/scitranslmed.aal3973

Zeng, S., Soetaert, K., Ravon, F., Vandeput, M., Bald, D., Kauffmann, J. M., & Fontaine, V. (2019). Isoniazid bactericidal activity involves electron transport chain perturbation. *Antimicrobial Agents and Chemotherapy*, *63*(3), 1–17. https://doi.org/10.1128/AAC.01841-18

Zimmermann, B., & Kohler, A. (2013). Optimizing savitzky-golay parameters for improving spectral resolution and quantification in infrared spectroscopy. *Applied Spectroscopy*, *67*(8), 892–902. https://doi.org/10.1366/12-06723

Zoffmann, S., Vercruysse, M., Benmansour, F., Maunz, A., Wolf, L., Blum Marti, R., & Prunotto, M. (2019). Machine learning-powered antibiotics phenotypic drug discovery. *Scientific Reports*, *9*(1), 1–14. https://doi.org/10.1038/s41598-019-39387-9

SUPPORTING INFORMATION

Additional Supporting Information may be found online in the supporting information tab for this article.

How to cite this article: Ribeiro da Cunha, B., Aleixo, S. M., Fonseca, L. P., & Calado, C. R. C. (2021). Fast identification of off-target liabilities in early antibiotic discovery with Fourier-transform infrared spectroscopy. *Biotechnology and Bioengineering*, 118, 4465–4476. https://doi.org/10.1002/bit.27915